DNA detection using a radio frequency biosensor with gold nanoparticles

Jui-Hung Chien[1], Ching-Hao Yang[1], Ping-Hei Chen[1], Chii-Rong Yang[2], Chin-Shen Lin[3], Huei Wang[3]

[1]Department of Mechanical Engineering, National Taiwan University, No. 1, Sec. 4, Roosevelt Rd., Taipei, Taiwan, 106, [2]Department of Mechatronic Engineering, National Taiwan Normal University, No. 162, Sec. 1, He-ping East Road, Taipei, Taiwan, 106, [3]Graduate Institute of Communication Engineering and Department of Electrical Engineering, National Taiwan University, No. 1, Sec. 4, Roosevelt Rd., Taipei, Taiwan, 106

TABLE OF CONTENTS

1. ABSTRACT

This study presents a novel method for DNA detection with multi-layer AuNPs to enhance overall detected sensitivity. This essay achieves not only an innovative radio-frequency biosensor but also a critical signal amplification methodology. Results show that bandwidth change for multi-layer AuNP with hybridization of DNA exceeds that for the double-layer AuNP up to 0.5 GHz. Furthermore, the detection limited of the developed biosensor for the DNA set employed in this essay is 10 pM. A single base-pair mutation of the wild-type target DNA could be distinguished from the perfect match target DNA at the melting temperature of $47^{o}C$ with a temperature controlling system. Experimental results of this study indicate that the proposed biosensor and the developed amplification methodology are successful. As health care becomes much more essential in modern life, this biosensor has potential applications in a screening kit for recognizing, sensing, and quantifying biomolecules in real samples.

2. INTRODUCTION

Reliable methods for detecting epidemic viral diseases in humans are under increasing demand in the genomic medicine field. Detecting a virus in a sample requires that the viral DNA must first be extracted, or complementary viral DNA obtained through reverse transcription of the RNA. During these purification or extraction processes, however, the final sample contains a much lower concentration of target analyte than the original sample (1). Therefore, enhancing sensitivity of the low concentration sample is critical for developing biosensors.

Numerous sensitive detection methods have been studied the past decade. Recently, DNA detection using functionalized nanoparticles (2, 3) has received increasing interest. Since received biosensor signals are not always strong enough for detection, amplification procedures are required either for the biomolecules or labeled reagents (4, 5).

Functionalizing particles with oligonucleotides along with the development of a series of practical biosensors has been recently reported. Metal nanoparticles such as gold or silver, due to their high surface areas, have excellent electric conduction abilities and are quite useful as catalysts. Hence, for the analyte of nucleic acid, the properties of hybridization with immobilization of nanostructure allow for the design of numerous assays.

Gold nanoparticles, among many practical methodologies however, are the most commonly used material as the bioreceptor label for its excellent affinity with biomolecules (6). The monolayer molecules of self-assembled gold nanoparticles help electron transfer across electrode surfaces. Colloidal Au (7) has been used to enhance DNA detection signals due to its ultrahigh surface areas, in optimizing the electrochemical DNA biosensor detection limit. These reports or papers present the outstanding electrical properties of gold nanoparticles for biomedical detection.

Substantial research groups have developed array-based electrical detection assays for DNA inspection (8, 9) since biosensors that detect target biomolecules through changes in electrical impedance with nanoparticle probes can have good detection sensitivities. The most popular amplification procedure strategy among those researches is silver enhancement to amplify electrical current. Detection speed increases with self-assembly gold nanoparticle multilayer (10) and fabricated nanogaps employed to improve electrical conductivity between electrode gaps.

Moreover the resistive sensors, other low frequency devices such as capacitive impedance biosensors are also widely investigated (11). The capacitors with gold nanoparticles through DNA hybridization formed on the interdigitated structures, and their gap impedance between two electrodes was measured for DNA detection (12). Most studies are devoted to developing DC or low frequency devices. Nevertheless, findings show that by comparing bio-conjugate dimensions with the biosensor, bio-conjugate dimension is much smaller than that of the biosensor. Hence capacitance changes are tiny (12) without applying additional enhancement procedures. High frequency response of the biomolecule-AuNP conjugate is also more intensive than the DC or low frequency response (13), and has better resolution at high frequency. However, few papers report biosensors utilizing advantageous high frequency characteristics. Therefore, this research proposes a novel scheme for detecting target DNA and an innovative signal amplification strategy at high frequency.

This paper considers two major aspects for biosensor development. The first applies biomolecule-AuNP conjugate response at high frequency on bio-sensing technology. A low-pass radio frequency filter (14, 15) is the proposed novel electronic device for DNA detection. The coplanar waveguide (CPW) micro-filter we have designed and used in our research can operated at high frequency, moreover, because it is a filter itself, it also has related applications in current telecommunication system (16,17).

The second objective is to develop a novel signal amplification scheme. Different from the time-consuming silver enhancement technology, self-assembled multilayer AuNPs are applied to specific binding of DNA primers to cause substantial amounts of AuNPs to attach to the biosensor. The idea of multilayer AuNPs is an improvement of our former work with double-layer assay (10). The current work, in addition to the double-layer gold, used a chemical compound hexandithiol, which has thiol groups (18) on both ends of the molecule to form the third layer gold nanoparticles. One end attaches to the double-layer AuNP surface and the other end can be used to establish the triple-layer AuNPs. Since the multiple layer gold nanoparticle is established, target protein signals can be largely amplified.

3. DESIGN AND FABRICATION OF THE COPLANAR WAVEGUIDE BIOSENSOR

3.1. Coplanar waveguide circuits

A conventional CPW consists of a center strip conductor with a semi-infinite ground plane on either side of a dielectric substrate (16). Compared with conventional microstrip lines, the CPW structures provide several advantages. 1. The fabrication process is largely simplified. 2. Since the ground plane and the circuits are on the same side, it eliminates the need via holes 3. It reduces radiation loss. Moreover, the cross-talk effect of two adjacent lines could be eliminated by a ground plane that divides these two adjacent lines. Therefore, the high density of CPW circuits offers many advantages for MIC as well as MMIC applications (19). This advantage differs from some microstrip periodic structures, where insertion loss and return loss vary depending upon where the top conductor is placed in reference to the periodically etched ground plane (20).

The MEMS design has a variety of structures on single side or double sides of the substrate. The choice of either one depends on device functionality and fabrication instrument facility. Since this work must reduce unstable conditions of devices, moving part designs are currently not a consideration. Hence CPW structures are the first choice in our study.

3.2. Dimensions of the periodic CPW circuits for filters

Dimensions of the proposed biosensor are illustrated, and the length and the width of proposed biosensor are 4.75 mm and 3.68 mm respectively (Figure 1). Dielectric substrate region is strongly affected by micro-strip line fields, therefore micro-strip field distribution characteristics are perturbed by slight periodic geometric variations of the designed filter. This investigation designs several continuities and discontinuities in the proposed filter to change effective capacitance and inductance along the CPW structure (21). Many parameters can be adjusted. For example, the center conductor in CPW circuits can be a narrow-shaped designed in order to enhance inductance per unit length. The two ground planes of the CPW line are designed closer to each other to increase capacitance beside the central conductor. By branching out the center strip conductor as the folk shaped structure, the proposed CPW circuits offer several bio-sensing advantages. The completely uniplanar geometries of the structures means the proposed
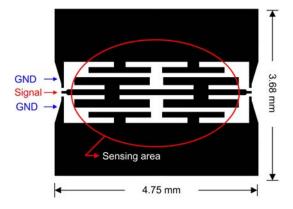
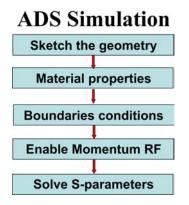**Figure 1.** Dimension of the proposed biosensor designed in AutoCad.

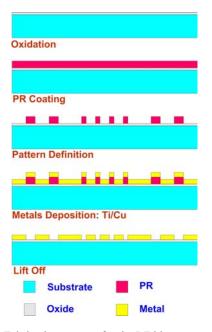**Figure 2.** Flow chart for the simulation process.

Figure 3. Fabrication process for the RF biosensor.

periodic CPW sensing circuits can be carried out by a very simple fabrication process implemented on one side of a dielectric substrate using standard etching techniques. No

additional procedures in the form of drills are required, and the smallest dimensions of the unit cells are still large enough such that no ion-beam process is required.

3.3. Electromagnetic simulation for the proposed biosensor

The designed miniaturized low-pass filter of coplanar type in this study was simulated in Agilent ADS (Figure 2). The biosensor geometry is drawn in the AutoCad commercial suits before input into the simulation tool. Air layer boundaries are fixed as a perfect conductor and copper is set as the perfect conductor metal for the planar circuit for simulation. The substrate used in this study is Pyrex glass. Therefore, corresponding values of dielectric layer material properties of the Pyrex glass are used in the simulation.

3.4. Materials for biosensor fabrication

Since the substrate demands a good dielectric property, the glass wafer chosen is Pyrex 7740, which has a relative dielectric constant of 3.8, a loss tangent of 3.3×10^{-4}, and a thickness of 600 μm. The photoresist AZ-4620 served as a proper photoresist for forming the micro mold for sputtering. Copper, with its proper conductivity of 5.8×10^{7} S/m, served as the main biosensor metal structure. Other chemical agents for stripping the photoresist and cleaning the wafer are commercial products of analytical grade.

3.5. Instruments for biosensor fabrication

The spin coater for providing a uniform spread of photoresist is the KYOWARIKEN Spin Coater (NTNU MOEMS Lab., Taiwan). The aligner employed for photoresist exposure is the mask aligner (USHIO, HB-25103BY-C, NTNU MOEMS Lab., Taiwan). The plasma enhanced chemical vapor deposition (PECVD) process is employed for depositing a silicon oxidation layer using Samco PD-220 (NTU NEMS center). Then the titanium seed layer is deposited using an ULVAC EGK-3M E-beam evaporator (NTU NEMS center). Finally the ultrasonic vibrator for releasing biosensors in the lift-off process is SY1200 purchased from the Ultrasonic Instrument Company.

3.6. Fabrication process

The fabrication process of the biosensor is depicted (Figure 3). Before the fabrication process, a silicon oxidation layer of 2000 Å was deposited on the wafer using the plasma enhanced chemical vapor deposition (PECVD) method (Samco PD-220). The photoresist AZ-4620 served as the metal deposition mold. The photoresist was a thickness of 15 μm; therefore, the spin process required two stages to complete (Figure 4A). The first stage was performed at 100 rpm for 30 sec, and the second stage was performed at 500 rpm for 30 sec. Before the soft bake process, the wafer remained at room temperature for 5 minutes to allow the liquid photoresist to spread. The metal deposition procedure began after the photoresist mold was complete. The total thickness was designed to be 5 μm to avoid skin depth effect. The 2000 Å seed layer material was titanium, deposited by an E-beam evaporator (ULVAC EGK-3M). Copper, with its proper conductivity of 5.8×10^{7} S/m, served as the main metal structure of the biosensor because metal conductivity is a critical issue in microwave device design (Figure 4B).

Table 1. Sequences of capture, probe, target and wild-type target strand with single base-pair mismatch

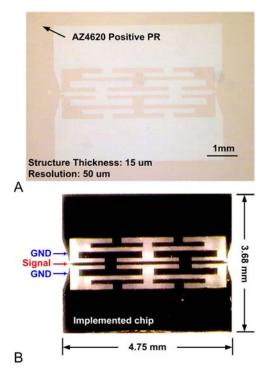| Name	Sequence
Capture DNA	3'-HS-AAAAAAAAAAACCTAATAACAAT-5'
Probe DNA	3'-TTATAACTATTCCTAAAAAAAAAAA-SH-5'
Target DNA	5'-GGATTAT**T**GTTAAATATTGATAAGGAT-3'
Wild Type Target DNA	5'-GGATTAT**C**GTTAAATATTGATAAGGAT-3'

Figure 4. Photographs of RF biosensor. (A) The photoresist on the substrate. (B) The implemented chip.

4. DNA DETECHTION

4.1. Principles of electrical detection for DNA hybridization

The DNA detection method by the radiofrequency biosensor is based on a selective process of specific surface bound hybridization. In the biosensor, single-strand captured DNA, suspended probe DNA, and complimentary target DNA in the solution are added and then hybridization occurs. This study employs a multilayer gold nanoparticle structure over the sensing areas rather than a monolayer with silver enhancement in order to obtain a measurable frequency shift of the biosensor after oligonucleotide hybridization. The multilayer gold nanoparticle procedure can be illustrated as follows (Figure 5). A self-assembly gold nanoparticle monolayer is immobilized on the surface of the biosensor gap by using the polymer chemical agent after biosensor fabrication. This chemical agent, 3-aminopropyltrimethoxysilane (APTMS), was coated on the substrate for enhancing the attachment of gold nanoparticles to the glass substrate. Secondly, the single strand thoil-modified captured DNA (tDNA) is added to the reaction region and immobilized onto the monolayer gold nanoparticle surface (Figure 5B). For the thiol group on the gold surface, sulfur has particular affinity for gold, with a binding energy in the range of 20–35 kcal/mol. An alkane with a thiol head group will stick to the gold surface and form an ordered assembly with the alkyl chains packing together due to van der Waals forces. Selective binding occurs among immobilized captured DNA, suspended probe DNA, and target DNA in the sample solution when those DNA sequences are placed on the biosensor (Figure 5C and Table 1). One end of the probe DNA is modified by thoil, but the other remains free. The last step includes rinsing the measured spot of the biosensor with a solution of phosphate-buffered saline (PBS) before adding gold nanoparticles. In case no hybridization among the target DNA (tDNA), captured DNA (cDNA), and probe DNA (pDNA) occurs, all suspended materials are then washed away. Therefore, no gold nanoparticles attach to the cDNA immobilized on the gold nanoparticle monolayer. Nevertheless, when complimentary hybridization takes place among the oligonulceotides, gold nanoparticles easily attach to the thoil-modified pDNA to establish the gold nanoparticle doublelayer for electrical detection (Figure 5D). Afterward, hexandithiol is employed as the linking agent to the double-layer AuNPs for amplification. The chemical compound hexandithiol has thiol on both ends of the molecule, so it can link two or more AuNP particles to form the network structure (Figure 5E). One end of the linking agent attaches to the double-layer AuNP surface and the other end reaches the triple-layer AuNPs.

The temperature gradient based method for detecting the single base-pair mismatch is based on the principle that bonding strength of partially denatured DNA is less than that of complete hybridization. This property allows for DNA separation by melting temperature. Adapting these methods for a single base-pair mismatch, or so-called the single nucleotide polymorphism (SNP) detection, uses two fragments: the target DNA that contains the SNP polymorphic site and the perfect match DNA fragment. The perfect match fragment is identical to the target DNA except potentially at the SNP polymorphic site, which is unknown in the target DNA. The fragments are denatured and then re-annealed.

Accurate prediction of the melting temperature of hybridization DNA strands is important. Since operation temperature of the experiments carried out in this assay should be carefully controlled, melting temperature of the DNA sequences employed needs to be calculated.

This study calculates the melting temperature (Tm) (21), instead of complex calculation, according to the following simplified equation (1):

$$T_m = 64.9 + 41.0 \times \left(\frac{yG + zC - 16.4}{wA + xT + yG + zC} \right)$$

(1)

where x, y, w and z are the number of the bases of T, G, A and C, respectively. The standard assumed conditions for this equation are a buffered solution of 50 mM Na$^+$ and 50 nM of oligonucleotide concentration, with a pH close to 7.0.
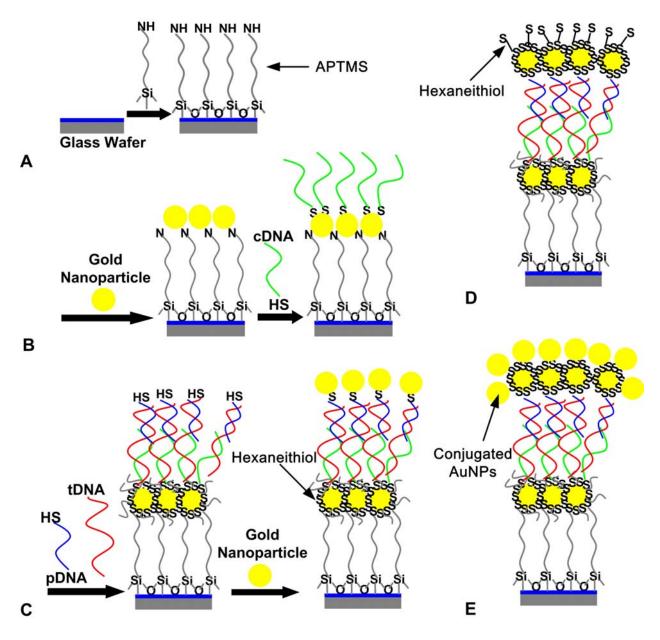
Figure 5. Procedure for establishing multilayer AuNPS: (A) The immobilization of the APTMS. (B) The immobilization of the capture DNA on the mono-layer AuNPs. (C) Addition of the target DNA and probe DNA with the double-layer AuNPs. (D) The addition of the 1,6-Hexanedithiol. (E) The immobilization of the Triple-layer AuNPs.

Sequences for this essay employed less than 27 bps. Due to sensing system factors developed, melting temperatures of the DNA sets can be derived. Because melting temperature for the perfect match is 48ºC and 46ºC for the single base pair mismatch, suitable operating temperature for our experiments is calculated to be 47ºC. The melting point detection process is depicted (Figure 6), and biochips are immersed in a PBS bath with a temperature heated to different temperature levels (Figure 6A). Then, AuNPs are added for establishing third-layer AuNPs after the suspended materials are removed (Figure 6B). Finally RF signal measurements are applied to the biochips (Figure 6C).

4.2. Chemicals and reagents

Some important reagents employed are acquired as follows: Acetone (100%, Mallincktodt), Milli-Q18 MΩ Distilled water (Millipore purification system), Hexanethiol (95%, Fluka), $HAuCl_4 \cdot 3H_2O$ (95%, Sigma), Phosphate Buffered Saline, PBS (Sigma), Sodium azide (99.5%, Sigma), NaH_2PO_4 (Sigma), Trisodium citrate (Sigma), 1,6-Hexanedithiol (95%, Fluka), 3-aminopropyltrimethoxysilane, APTMS (Sigma). All other chemicals were of commercially available analytical reagent grade.
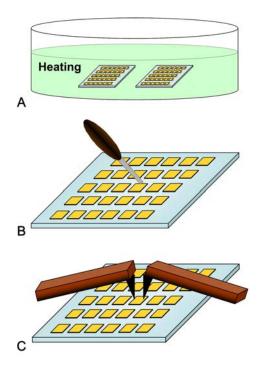
Figure 6. Procedure of the SNP detection. (A) Immersion of the biochip in a PBS bath of which the temperature is heated up to different temperature levels. (B) Addition of AuNPs for establishing third-layer AuNPs. (C) Measurements of the RF signals form the biochips.

4.3. Solutions preparation

The washing buffer was a solution of PBS containing 0.05% Tween 20. The PBS used was a solution of pH 7.4 containing 150mM NaCl and 10mM NaH_2PO_4. The probe DNA and captured DNA are diluted to 0.1 μM for immoblilization.

4.4. Preparation of gold nanoparticles (AuNPs)

A 4 mL of 1% (w/w) $HAuCl_4$ solution was added to 400 mL of distilled water, and then it was heated to boiling for 30 minutes. The 1% (w/w) sodium citrate solution of 8 mL was then added to the boiling solution. The solution changed color immediately from purple to dark red and was stirred to cool to avoid aggregation. The solution was adjusted to pH 9.0 by 0.1 M K_2CO_3. Afterwards, the AuNPs solution was stored in a 4°C refrigerator.

4.5. Establishment of monolayer AuNPs

Gold nanoparticles (AuNPs) are first essentially prepared to modify the DNA. The functionalized sensing circuits on the glass wafer are immersed in the gold nanoparticle (12-nm diameter) solution for 8-12 hours, then rinsed with distilled water and dried under N_2.

4.6. Establishment of double-layer AuNPs

The thiolated captured DNA is afterward immobilized onto the top surface of the AuNPs monolayer by spotting a 10mM HEPES / 5 mM EDTA buffer solution of appropriate alkylthiol-modified oligonucleotide (0.1 μM) on the chip by manual pipetting. After spotting captured DNA, the sensing tag is stored to allow coupling between gold

nanoparticles and alkylthiol-modified captured DNA. Finally, the DNA-functionalized sensing tag is washed with ethanol and water and blown dry in N_2. Then, the chip is immersed into a 10 mM HEPES / 5 mM EDTA buffer solution of target DNA (1 nM) and rinsed with a 0.3 M PBS solution. Finally, the sensing tag is immersed in a 0.3 M PBS solution of 12-nm diameter gold particles to establish the second layer of AuNPs and rinsed with a 0.3 M PBS solution again to wash the suspended materials away. This procedure is essential and critical because the added gold nanoparticles cannot attach to the free end (no thiolated modification) of captured DNA to form the second layer of AuNPs. If hybridization occurs among capture, target, and probe DNA, the added gold nanoparticles attach to the thoilated end of probe DNA to form a second layer of AuNPs. If no hybridization occurs in the solution, both target DNA and probe DNA are rinsed away.

4.7. Establishment of triple-layer AuNPs

After rinsing the biosensor with the washing buffer to remove the un-reacted probe DNA –Au, a 0.5mM hexandithiol solution was added on the sensing surface for 2 hours of incubation at room temperature. The chemical compound hexandithiol (Fluka Chemical Co.) has thiol on both ends of the molecule. One end attaches to the double-layer AuNP surface and the other end can be used to establish triple-layer AuNPs. Then the washing buffer to remove the un-reacted blocking agent rinses the biosensor again. Results for comparing the difference of double-layer AuNPs and triple-layer AuNPs are illustrated (Figure 8).

5. RESULTS AND DISCUSSIONS

5.1. Simulated results of the biosensor

The MEMS biosensor designed in this research with the slow-wave transmission line is simulated in Agilent ADS 2004A. The MEMS low-pass filter is characterized to determine microwave characteristics. The scattering parameter S_{21} simulated of the pass band of the designed filter is determined (Figure 7). The 3-dB bandwith of the biosensor without AuNPs and analyte is clearly about 19 GHz in the simulated result. On the other hand, the S_{21} at the low frequency band of this biosensor around 0GHz - 19 GHz is obviously very close to 0 dB. This means that this filter designed is very successful since the low frequency signals can almost pass the filter and only a few signals are lost during transmission.

5.2. On-wafer measured results of the biosensor

The network analyzer and microprobe station in this section characterize the scattering parameters. Wafers or chips are put on the sample stage and fixed by the pumping suction whenever the measurement is in progress. The vector network analyzer is Aligent 8722ES (SOC Technology Center, ITRI) that is used to measure S-parameter of the low-pass filter of the biosensors.

The measured signal response of DNA detection on the proposed biosensor clearly shows that the electromagnetic characteristics of this biosensor are a low-pass filter, and the 3-dB bandwidth is around 18.5 – 19.7 GHz (Figure 8). Signal smoothness around 0 GHz to 18.5 GHz means that signal loss
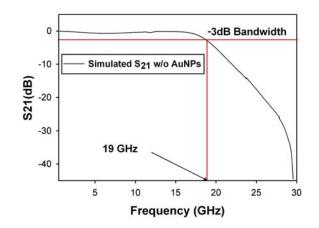
Figure 7. Simulation result of the S_{21} response of the proposed biosensor.
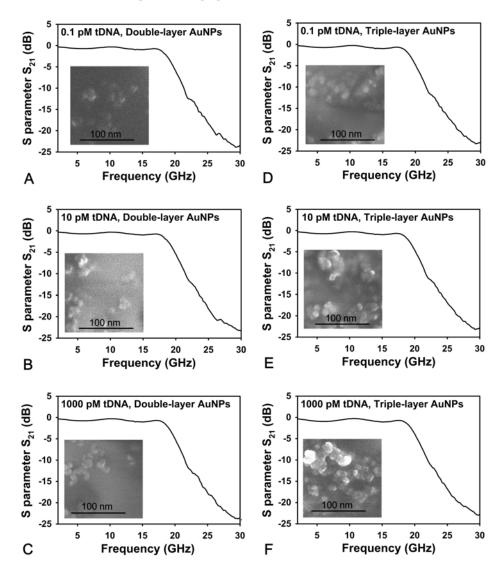

Figure 8. On-wafer measured S_{21} results of multi-layer AuNPs on the biochips at different concentrations of target DNA. Inset show the corresponding SEM micrographs of the biochips of multi-layer AuNPs. The left column A-C shows the double-layer AuNPs, while the right column D-F shows the triple-layer AuNPs.
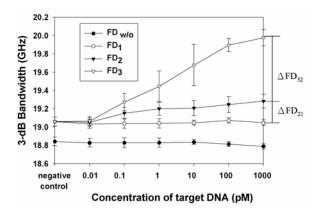
Figure 9. Measurement results of the -3dB bandwidth at different target DNA concentrations.
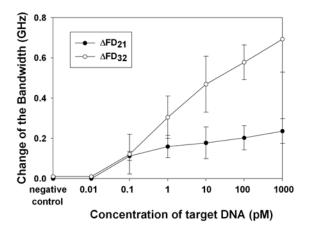

Figure 10. The results of 3-dB bandwidth change of DNA detection.
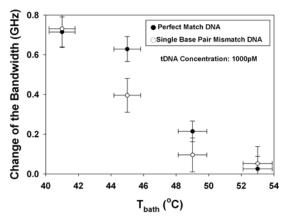

Figure 11. Variation of change in 3-dB bandwidth with the PBS bath temperature for distinguishing between perfect match DNA and single base-pair mismatch DNA.

at the pass band of this filter is very small. Comparing the SEM micrographs with the measured curves, the variation of the 3-dB bandwidth is proportional to distributed density of the AuNPs that shows in the SEM micrographs, and the

change of the 3-dB bandwidth is around 0.1-0.8 GHz. The 3-dB bandwidth of the simulated results and that of the measured results are very close, meaning that the prediction of the electromagnetic characteristics is correct. However more noise is obviously present at high frequency. Since signals higher than the 3-dB bandwidth are blocked from transmission, the noise at such band is relatively stronger than the noise at low frequency.

5.3. Frequency shift of the 3-dB bandwidth

The variation in the S-parameter values before and after the establishment of multi-layer gold nanoparticles is used to determine whether the target DNA exists in the test sample or not. FD_1, FD_2 and FD_3 denote the values of measured 3-dB bandwidth after the mono-layer, double-layer, and triple-layer of AuNPs with DNA are established respectively while $FD_{w/o}$ denotes the measured 3-dB bandwidth of the biosensor without immobilized AuNP-DNA structure. Here, the definitions of ΔFD_{21} and ΔFD_{32} can be described using the equations as follows,

$$\Delta FD_{21} = FD_2 - FD_1 \qquad (2)$$
$$\Delta FD_{32} = FD_3 - FD_2 \qquad (3)$$

The 3-dB bandwidth of the low-pass filters is changed with different DNA concentrations (Figure 9). If the -3dB bandwidth of the mono-layer and double-layer sample are used as references, the frequency shift of the 3-dB bandwidth with different DNA concentrations can be plotted as the curve ΔF_{21} and ΔF_{32} respectively (Figure 10). The 3-dB bandwidths do not change significantly as those without AuNPs and mono-layer of AuNPs are established. However, the 3-dB bandwidth obviously changes when multilayer AuNPs are applied. A higher DNA concentration results in larger 3-dB bandwidth frequency shift when using multilayer AuNPs. Error bars show the 95% confidence intervals of measured results (Figure 9, 10). The sensitivity, from the curve of the double-layer AuNPs should be defined as 10pM of DNA solution as it can be distinguishable from double-layer and triple-layer enhancement (Figure 10). However, a 0.1pM and 1pM of DNA solution can be detected after the triple-layer AuNPs are completely formed but not easy to read. Detection sensitivity can be enhanced with the triple-layer AuNPs.

This work employs a thermal box with temperature controlling systems for the single base pair mismatch detection. Since the calculated melting temperature is 46°C - 48°C, the experiments are conducted under temperatures of 41°C, 45°C, 49°C and 53°C to test for hybridization melting. Analyte concentration for perfect match and single base pair mismatch oligonucleotides is 1μM. We can sketch the plot of change of 3-dB bandwidth v.s. the PBS bath temperature (T_{bath}) to detect if the single-base pair mismatch exists (Figure 11). The 43°C and 53°C results clearly indicate that the single base-pair mismatch and perfect match DNA can be distinguished from the -3dB bandwidth change.

6. CONCLUSIONS

In conclusion, this study presents a novel detection method for DNA with multi-layer AuNPs to enhance overall detection sensitivity. Multilayer AuNPs in

the biosensor gaps can alter sensor electromagnetic behaviors, and thus change sensing circuit bandwidth. Therefore, circuit bandwidth is the critical factor indicating analyte existence in the sample solution. The following conclusions are drawn from the measured results.

1. Detection limit of developed biosensor for the DNA set in this essay is 10pM.

2. Bandwidth change for multi-layer AuNP, formed by complementary target DNA, exceeds that of the double-layer AuNP by 0.5 GHz.

3. The single mutation of target DNA could be distinguished approximately for the tested target DNA with a length of 27 bps with a temperature controlling system.

Establishing an AuNPs network in the micro-scale gaps of the proposed biosensor can greatly improve sensing abilities compared with traditional chemical processes. The biosensor designed in this study operates at high frequency, thus providing better resolution for tiny changes in frequency shift. The experimental results in this study indicate that this biosensor and chemical detection methodology are successful. As health care becomes more essential in modern life, this biosensor has potential applications in a screening kit for recognizing, sensing, and quantifying biomolecules in real samples.

8. REFERENCES

1. Minunni, M., Tombelli, S., Scielzi, R., Mannelli, I., Mascini, M. and Gaudiano, C.: Detection of β-thalassemia by a DNA piezoelectric biosensor coupled with polymerase chain reaction. *Anal Chim Acta* 481, 55-64 (2003)
2. Cai, H., Xu, C., He, P. and Fang, Y.: Colloid Au-enhanced DNA immobilization for the electrochemical detection of sequence-specific DNA. *J Electroanal Chem* 510, 78-85 (2001)
3. Taton, T. A., Mucic, R. C., Mirkin, C. A., Letsinger, R. L.: The DNA-Mediated Formation of Supramolecular Mano- and Multilayered Nanoparticle Structures. *J Am Chem Soc*, 122, 6305-6306 (2000)
4. Gooding, J. J.: Electrochemical DNA hybridization biosensors. *Electroanalysis* 14, 1149-1156 (2002)
5. Drummond, T., Hill, M. and Barton, J.: Electrochemical DNA biosensors. *Nat Biotechnol* 21, 1192-1199 (2003)
6. Wang, J.: Electrochemical nucleic acid biosensors. *Anal Chim Acta* 288, 205-214 (1994)
7. Lu, M., Li, X. H., Yu, B. Z., Li, H. L.: Electrochemical behavior of Au colloidal electrode through layer-by-layer self-assembly. *J Colloid Interface Sci* 123, 376-382 (2001)
8. Park, S. J., Taton, T. A. and Mirkin, C. A.: Array-based electrical detection of DNA with nanoparticle probes. *Science* 295, 1503-1506 (2002)
9. Berney, H., West, J., Haefile, E., Alderman, J., Lane, W., Collins, J.K.: A DNA diagnostic biosensor: development, characterization and performance. *Sens Actuators B Chem* 68, 100-108 (2000)
10. Tsai, C. Y., Tsai, Y. H., Pun, C. C., Chan, B., Luh, T. Y., Chen, C. C., Ko, F. H., Chen, P. J. and Chen, P. H.: Electrical Detection of DNA Hybridization with Multilayer Gold Nanoparticles between Nanogap Electrodes. *Microsyst Technol* 11, 91-96 (2005)
11. Berggren, C., Bjanason, B., Johansson, G.: An immunological Interleukine-6 capacitive biosensor using perturbation with a potentiostatic step. *Biosens Bioelectron* 13, 1061-1068 (1998)
12. Moreno-Hagelsieb, L., Lobert, P.E., Pampin, R., Bourgeois, D., Remacle, J., Flandre, D.: Sensitive DNA electrical detection based on interdigitated Al/Al_2O_3 microelectrodes. *Sens Actuators B Chem* 98, 269-274 (2004)
13. Kim, Y. I., Park, T. S., Kang, J. H., Lee, M. C., Kim, J. T., Park, J. H., Baik, H. K.: Biosensors for label free detection based on RF and MEMS technology. *Sens Actuators B Chem* 119, 592-599 (2006)
14. Goeruer, A., Karpuz, C., and Alkan, M.: Characteristics of periodically loaded CPW structures. *IEEE Microwave Guided Wave Lett* 8, 278-280 (1998)
15. Yang, F. R., Qian, Y., Coccioli, R., and Itoh, I.: A novel low-loss slow-wave microstrip structure. *IEEE Microwave Guided Wave Lett* 8, 372-374 (1998)
16. Sawata, S., Kai, E., Ikebukuro, K., Iida, T., Honda, T. and Karube, I.: Application of peptide nucleic acid to the direct detection of deoxyribonucleic acid amplified by polymerase chain reaction. *Biosens Bioelectron* 14, 397-404 (1999)
17. Wu, K. and Vahldieck, R.: Hybrid-mode analysis of homogeneously and inhomogeneously doped low-loss slow-wave coplanar transmission lines. *IEEE Trans Microw Theory Tech* 39, 1348-1360 (1991)
18. Faucheux, N., Schweiss, R., Lützow, K., Werner, C., Groth, T.: Self-assembled monolayers with different terminating groups as model substrates for cell adhesion studies. *Biomaterials* 25, 2721-2730 (2004)
19. Goeruer, A.: A novel coplanar slow-wave structure. *IEEE Microwave Guided Wave Lett* 4, 86-88 (1994)
20. Simons, R. N.: Coplanar waveguide circuits, components, and systems. *Wiley Interscience*, NY (2001)
21. Sor, J., Qian, Y., Itoh, T.: Miniature low-loss CPW periodic structures for filter applications. *IEEE Trans Microw Theory Tech* 49, 2336-2341 (2001)
22. Marmur, J. and Doty, P.: Determination of the base composition of deoxyribonucleic acid from its thermal denaturation temperature. *J Mol Biol* 5, 109-118 (1962)

Send correspondence to: Dr. Ping-Hei Chen, Department of Mechanical Engineering, National Taiwan University, No. 1, Sec. 4, Roosevelt Rd., Taipei, Taiwan 10617, R.O.C., Tel: 886-2-23670781, Fax: 886-2-23631755, E-mail: phchen@ntu.edu.

http://www.bioscience.org/current/vol13.htm